Electronic Supplementary Information (ESI)

[PyH][{TpMo(μ_3-S)$_4$Cu$_3$}$_4$(μ_{12}-I)]: A Unique Tetracubane Cluster Derived from the S-S Cleavage and the Iodide Template Effects and its Enhanced NLO Performances†

Zhen-Hong Wei,[a,b] Chun-Yan Ni,[a] Hong-Xi Li,[a] Zhi-Gang Ren,[a] Zhen-Rong Sun,[c] and Jian-Ping Lang*[a,b]

[a] College of Chemistry, Chemical Engineering and Materials Science, Soochow University, Suzhou 215123, Jiangsu, P. R. China.

[b] State Key Laboratory of Organometallic Chemistry, Shanghai Institute of Organic Chemistry, Chinese Academy of Sciences, Shanghai 200032, P. R. China

[c] Department of Physics, East China Normal University, Shanghai 200062, P. R. China

Table of Contents

Experimental Section

General. Solvents like DMF and MeCN were dried over CaH_2 and distilled in vacuo. All chemicals and reagents were obtained from commercial sources and used as received. Compound **1** was prepared according to the literature procedures previously reported.[1] The elemental analyses for C, H, N were performed on a Carlo-Erba CHNO-S microanalyzer. The IR spectra were recorded on a Varian 1000 FT-IR spectrometer as KBr disks (4000-400 cm^{-1}). UV-vis spectra were measured on a Varian 50 UV-visible spectrophotometer. The emission and excitation spectra were measured on a Varian Cary Elipse fluorescence spectrophotometer.

Synthesis of 2. To a solution of **1** (60 mg, 0.1 mmol) in MeCN (15 mL) was added CuI (57 mg, 0.3 mmol). The mixture was stirred for 0.5 h and then filtered. Et_2O (4 mL) was carefully layered onto the dark green filtrate. Dark green blocks of **2**·3.5MeCN were formed in one week, which were collected by filtration, washed with Et_2O, and dried in air. Yield: 97 mg (75% based on **1**). Anal. Calcd. for $C_{41}H_{70.5}B_2Cu_7I_7Mo_2N_{17.5}S_6$: C, 19.33; H, 2.79; N, 9.62. Found: C, 19.46; H, 2.60; N, 9.36. IR (KBr disk): 2977 (m), 2924 (m), 2563 (w), 2094 (s), 1610 (m), 1547 (s), 1483 (m), 1436 (s), 1349 (m), 1222 (s), 1034 (s), 1000 (m), 860 (m), 753 (m), 724 (s), 692 (s), 651 (s), 478 (w), 430 (w) cm^{-1}. UV-Vis (DMF, λ_{max} (nm (ε M^{-1} cm^{-1}))): 634 (3340). ^{1}H NMR (400 MHz, DMSO-d_6): δ 1.01-1.16 (t, 12H, CH_2CH_3), 3.15-3.22 (q, 8H, CH_2CH_3), 5.73 (s, 1H, B-H), 6.39 (s, 3H, CH in Tp), 7.95 (s, 3H, CH in Tp), 8.10 (s, 3H, CH in Tp).

Synthesis of 3. To a solution of **1** (60 mg, 0.1 mmol) in pyridine (10 mL) was added CuI (57 mg, 0.3 mmol). The mixture was stirred at ambient temperature for 1 h. The resulting dark brown solution was concentrated and filtered. Et_2O (4 mL) was carefully layered onto the filtrate to form dark red blocks of **3**·Et_2O in two weeks, which were collected by filtration, washed with Et_2O, and dried in air. Yield: 26 mg (36% based on **1**). Anal. Calcd. for $C_{45}H_{56}B_4Cu_{12}IMo_4N_{25}OS_{16}$: C, 18.92; H, 3.41; N, 12.85. Found: C, 19.56; H, 3.60; N, 12.76. IR (KBr disk): 2979

(m), 2925 (m), 2559 (w), 2091 (s), 1608 (m), 1546 (s), 1482 (m), 1437 (s), 1348 (m), 1221 (s), 1033 (s), 999 (m), 862 (m), 751 (m), 725 (s), 690 (s), 654 (s), 476 (w), 433 (w) cm^{-1}. UV-Vis (DMF, λ_{max} (nm (ε M^{-1} cm^{-1}))): 649 (3450). ^{1}H NMR (400 MHz, DMSO-d_6): δ 5.73 (s, 4H, B-H), 6.41 (s, 12H, CH in Tp), 7.36 (d, 2H, Py), 7.78 (dq, 1H, Py), 8.01 (s, 12H, CH in Tp), 8.12 (s, 12H, CH in Tp), 8.56 (d, 2H, Py). The N-H proton of PyH^+ was not located.

Characterization of 2 and 3. The elemental analysis for **2** and **3** was consistent with their chemical formula. X-ray fluorescence analysis showed the correct ratio for Mo : S : Cu : I = 2 : 6 : 7 : 7 for **2**, and Mo : S : Cu : I = 4 : 12 : 12 : 1 for **3**. The ^{1}H NMR spectra of **3** in DMSO-d_6 at ambient temperature displayed the correct B-H/pyrazolyl methane/PyH proton ratio for the Tp moiety and the pyridinium.

X-ray Crystallographic Study. Diffraction intensities of **2**·3.5MeCN and **3**·Et_2O were collected on a Rigaku Mercury CCD X-ray diffractometer (Mo Kα, λ = 0.71073 Å). The single crystals of **2**·3.5MeCN and **3**·Et_2O were mounted at the top of a glass fiber with grease at 223 K in a stream of gaseous nitrogen. Cell parameters were refined on all observed reflections by using the program *CrystalClear* (Rigaku and MSc, Ver. 1.3, 2001). The collected data were reduced by the program *CrystalClear*, and an absorption correction (multi-scan) was applied. The reflection data were also corrected for Lorentz and polarization effects.

The crystal structures of **2**·3.5MeCN and **3**·Et_2O were solved by either direct methods[2] and refined on F^2 by full-matrix least-squares techniques with *SHELXTL-97* program. For **2**·3.5MeCN, because of the evaporation of solvated molecules, the site-occupation factor of two MeCN solvated molecules (C18, C19 and N8; C22, C23 and N10 atoms) was fixed at 0.25 and 0.5, respectively. Also in refining MeCN molecules, the restrained parameters to fix the bonds C18-C19, C22-N10, C20-C21, C23-N10 and to equal the U values of atoms N10, C22, C23 and C18, C19 N8 were applied. One pyrazole rings were disordered and the U values atoms C7, C8, C9 were refined using restrained parameters. For **3**·Et_2O, the pyridyl group of N7 and C10-C14 was treated as a rigid group with

site-occupancy factor of 0.25. Due to the partial evaporation of the solvated Et_2O molecules, the site-occupation factor for O1, C15 and C16 was fixed at 0.5. All non-hydrogen atoms, except for those of the MeCN solvated molecules in **2**·3.5MeCN and the protonated pyridine and Et_2O solvated molecules in **3**·Et_2O, were refined anisotropically. Hydrogen atoms including the B-H and the N-H in pyridine group were placed in geometrically idealized positions (C-H = 0.98 Å, with U_{iso}(H) =1.5U_{eq}(C) for methyl groups; C-H = 0.99 Å, with U_{iso}(H) =1.2U_{eq}(C) for methylene groups; C-H = 0.95 Å, with U_{iso}(H) =1.2U_{eq}(C) for aromatic rings) and constrained to ride on their parent atoms.

Third-Order NLO Measurements of 2 and 3. The solutions of **2** (4.9×10^{-5} M) and **3** (3.6×10^{-5} M) in DMF were placed in a 1.5 mm quartz cuvette for the third-order NLO measurements. These six compounds were stable toward air and laser light under experimental conditions. As a reference, the optical nonlinearity of the standard sample CS_2 was also observed. The third-order NLO properties were measured using femtosecond DFWM technique with a Ti:Sapphire laser (Spectra-physics Spitfire Amplifier). The pulse width was determined to be 80 fs on a SSA25 autocorrelator. The operating wavelength was centered at 800 nm. The repetition rate of the pulses was 1 kHz. During the measurement the laser was very stable (rms < 0.1%). The input beam was split into two beams k_1 and k_2 with nearly equal energy by use of a beam splitter (BS) and then focused on a plot of the sample. The beam k_2 passed through a delay line derived by a stepping motor in order that the optical path length difference between the k_2 and k_1 beams could be adjusted during the measurement. The angle between the beams k_1 and k_2 were about 5°. When k_1 and k_2 were overlapped spatially in the sample, the generated signal beam k_3 passed through an aperture, recorded by a photodiode and then analyzed by a lock-in amplifier and computer.

Details of the equations used in calculations of Third-order NLO properties. The third-order NLO susceptibility $\chi^{(3)}$ is measured *via* a comparison with that of a reference sample CS_2, calculated from the DFWM signal (I), the linear refractive index (n), the sample thickness (L) and absorption correction factor using eq. 1:[3]

$$\chi_s^{(3)} = \left(\frac{I_s}{I_r}\right)^{1/2} \cdot \frac{L_r}{L_s} \cdot \left(\frac{n_s}{n_r}\right)^2 \cdot \frac{\alpha \cdot L \cdot \exp(\alpha L/2)}{1-\exp(-\alpha L)} \cdot \chi_r^{(3)} \qquad (1)$$

where the subscripts "*s*" and "*r*" represent the parameters for the sample and CS_2. And α is the linear absorption coefficient. The last fraction comes from the sample absorption and equals to 1 while the sample has no absorption around the employed laser wavelength. The values of $\chi_r^{(3)}$ and n_r for CS_2 are 6.7×10^{-14} esu and 1.632, respectively.[4]

The third-order nonlinear refractive index n_2 in isotropic media is estimated through eq. 2:[5]

$$n_2(esu) = \frac{12\pi\chi^{(3)}}{n^2} \qquad (2)$$

where n is the linear refractive index of the solution.

The second-order hyperpolarizability γ of a molecule in isotropic media is related to the solution $\chi^{(3)}$ by Equation (3):[6]

$$\gamma = \frac{\chi^{(3)}}{Nf^4} \qquad (3)$$

where N is the number density of the solute per milliliter, and f^4 is the local field correction factor which is $[(n^2 + 2)/3]^4$ (n is the linear refractive index of solution).

References

1. H. Seino, Y. Arai, N. Iwata, S. Nagao, Y. Mizobe, M. Hidai, *Inorg. Chem*., **2001**, *40*, 1677.

2. (a) G. M. Sheldrick, *SHELXS-97, Program for Solution of Crystal Structures*; University of Göttingen: Göttingen, Germany, 1997. (b) G. M. Sheldrick, *SHELXL-97, Program for Refinement of Crystal Structures*; University of Göttingen, Göttingen, Germany, 1997.

3. Y, Yang, M. Samoc and P. N. Prasad, *J. Chem. Phys*., **1991**, *94*, 5282.

4. M. E. Orezyk, M. Samoc, J. Swiatkiewicz and P. N. Prasad, *J. Chem. Phys*., **1993**, *98*, 2524.

5. S. A. Jenekhe, S. K. Lo and S. R. Flom, *Appl. Phys. Lett*., **1989**, *54*, 2524.

6. B. K. Mandal, B. Bihari, A. K. Sinha, M. Kamath and L. Chen, *Appl. Phys. Lett*., **1995**, *66*, 932.

Table S1. Summary of crystallographic data for **2**·3.5MeCN and **3**·Et_2O.

Compound	**2**·3.5MeCN	**3**·Et_2O
Empirical Formula	$C_{41}H_{70.5}B_2Cu_7I_7Mo_2N_{17.5}S_6$	$C_{45}H_{56}B_4Cu_{12}IMo_4N_{25}OS_{16}$
Formula Weight	2547.72	2792.77
Crystal System	monoclinic	orthorhombic
Space Group	*C*2	*Ccca*
a (Å)	21.451(4)	15.803(3)
b (Å)	14.204(3)	27.090(5)
c (Å)	17.038(3)	23.606(5)
β (°)	124.80(3)	
V (Å^3)	4262.9(15)	10106(3)
Z	2	4
ρ_{calc} (g/cm^3)	1.985	1.836
F(000)	2406	5416
μ (MoKα,mm^{-1})	4.712	3.622
Total reflections	17881	16459
Unique reflection	9166 (R_{int} = 0.0462)	4444 (R_{int} = 0.0355)
No. observations	5796 ($I > 2.00\sigma(I)$)	4138 ($I > 2.00\sigma(I)$)
No. parameters	345	239
R^a	0.0387	0.0654
$R_w{}^b$	0.1015	0.1924
GOF^c	0.944	1.246

[a] $R = \Sigma||F_o|-|F_c||/\Sigma|F_o|$. [b] $R_w = \{\Sigma w(F_o^2-F_c^2)^2/\Sigma w(F_o^2)^2\}^{1/2}$. [c] GOF = $\{\Sigma w((F_o^2-F_c^2)^2)/(n-p)\}^{1/2}$, where *M* is the number of reflections and *N* is the number of parameters.

Table S2. Selected bond lengths (Å) and angles (°) for **2** and **3**.

Compound **2**

I4-Cu4	2.6750(14)	I4-Cu3	2.9231(16)	I4-Cu2	3.0004(16)
I4-Cu1	3.059(2)	I2-Cu2	2.4934(16)	I2-Cu4	2.6646(17)
I3-Cu3	2.5186(17)	I1-Cu1	2.4859(15)	Mo1-N2	2.243(8)
Mo1-N4	2.242(9)	Mo1-N6	2.244(8)	Mo1-S2	2.289(3)
Mo1-S3	2.293(3)	Mo1-S1	2.297(3)	Mo1···Cu2	2.6349(17)
Mo1···Cu1	2.6370(15)	Mo1···Cu3	2.6531(19)	Cu3-S2	2.226(3)
Cu3-S3	2.229(3)	Cu3-Cu2	2.980(2)	Cu3···Cu1	3.028(2)
Cu2-S1	2.227(3)	Cu2 S2	2.227(3)	Cu2···Cu4	2.9342(19)
Cu1-S1	2.208(3)	Cu1-S3	2.213(3)	Cu4-I2A	2.6646(17)
Cu4-I4A	2.6750(14)	Cu4···Cu2A	2.9342(19)		
Cu4-I4-Cu3	91.88(5)	Cu4-I4-Cu2	61.95(4)	Cu3-I4-Cu2	60.38(4)
Cu4-I4-Cu1	123.12(4)	Cu3-I4-Cu1	60.77(4)	Cu2-I4-Cu1	61.18(4)
Cu2-I2-Cu4	69.25(6)	Cu3-I3-Cu3A	106.23(8)	S2-Mo1-S3	104.64(10)
S2-Mo1-S1	105.73(10)	S3-Mo1-S1	104.96(10)	S2-Cu3-S3	108.94(11)
S2-Cu3-I3	116.92(9)	S3-Cu3-I3	118.84(10)	S2-Cu3-I4	104.48(9)
S3-Cu3-I4	103.81(9)	I3-Cu3-I4	101.55(5)	S1-Cu2-S2	110.31(11)
S1-Cu2-I2	118.53(10)	S2-Cu2-I2	119.39(9)	S1-Cu2-I4	100.88(9)
S2-Cu2-I4	102.06(9)	I2-Cu2-I4	101.67(5)	S1-Cu1-S3	110.86(11)
S1-Cu1-I1	116.93(9)	S3-Cu1-I1	118.83(9)	S1-Cu1-I4	99.60(9)
S3-Cu1-I4	100.10(8)	I1-Cu1-I4	106.96(5)	I2-Cu4-I2A	107.00(9)

I2-Cu4-I4A	110.87(3)	I2-Cu4-I4	106.26(4)	I2A-Cu4-I4A	106.26(4)
I2-Cu4-I4A	110.87(3)	I4-Cu4-I4A	115.34(9)	Cu1-S3-Cu3	85.96(11)
Cu1-S3-Mo1	71.63(9)	Cu3-S3-Mo1	71.84(9)	Cu1-S1-Cu2	88.13(10)
Cu1-S1-Mo1	71.64(9)	Cu2-S1-Mo1	71.23(9)	Cu3-S2-Cu2	84.00(10)
Cu3-S2-Mo1	71.97(9)	Cu2-S2-Mo1	71.38(9)		

Compound **3**

Mo1-N4	2.268(7)	Mo1-N2	2.271(8)	Mo1-N6	2.275(8)
Mo1-S3	2.301(2)	Mo1-S2	2.314(2)	Mo1-S1	2.318(2)
Mo1···Cu2	2.6438(14)	Mo1···Cu1	2.6551(14)	Mo1···Cu3	2.6794(14)
Cu3-S3	2.224(3)	Cu3-S2	2.234(3)	Cu3-S4	2.238(3)
Cu1-S4A	2.215(2)	Cu1-S3	2.216(2)	Cu1-S1	2.232(3)
Cu2-S4B	2.201(2)	Cu2-S2	2.216(3)	Cu2-S1	2.227(3)
S3-Mo1-S2	104.55(9)	S3-Mo1-S1	104.89(9)	S2-Mo1-S1	104.88(9)
S3-Cu3-S2	109.92(10)	S3-Cu3-S4	122.49(9)	S2-Cu3-S4	124.38(10)
S4A-Cu1-S3	120.09(10)	S4A-Cu1-S1	125.77(10)	S3-Cu1-S1	110.80(9)
S4B-Cu2-S2	122.06(10)	S4B-Cu2-S1	124.78(10)	S2-Cu2-S1	111.47(9)
Cu2-S1-Cu1	87.99(9)	Cu2-S1-Mo1	71.10(8)	Cu1-S1-Mo1	71.36(7)
Cu1-S3-Cu3	90.15(9)	Cu1-S3-Mo1	71.96(7)	Cu3-S3-Mo1	72.58(8)
Cu2-S2-Cu3	89.27(9)	Cu2-S2-Mo1	71.38(8)	Cu3-S2-Mo1	72.17(8)
Cu2A-S4-Cu1B	93.38(9)	Cu2-S4B-Cu3	96.38(9)	Cu1-S4A-Cu3	94.99(9)

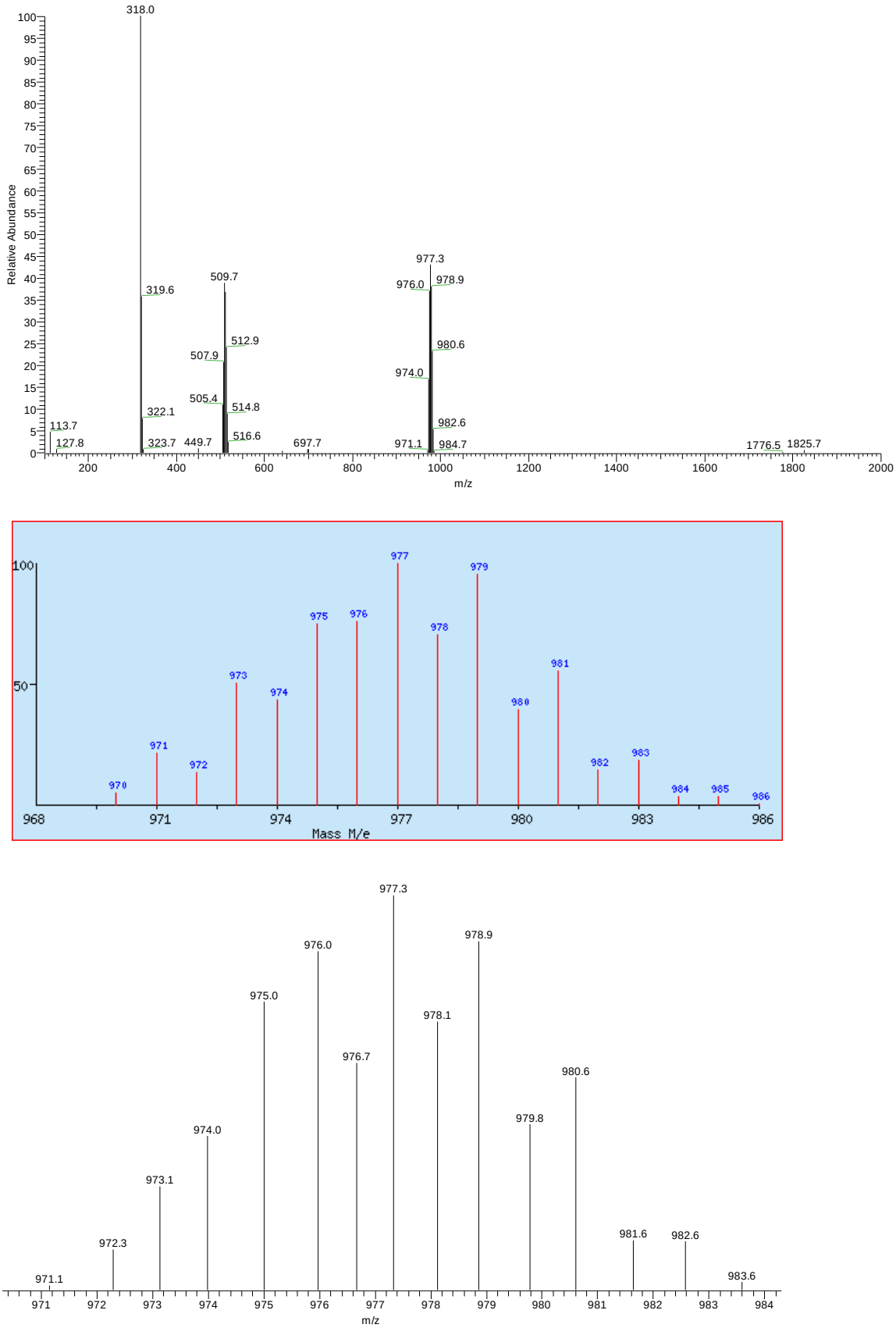

Figure S1. The negative-ion ESI mass spectrum of **2** (upper), and the calculated (middle) and the observed (lower) isotopic patterns for $[TpMoS_3(CuI)_3]^-$ anion.

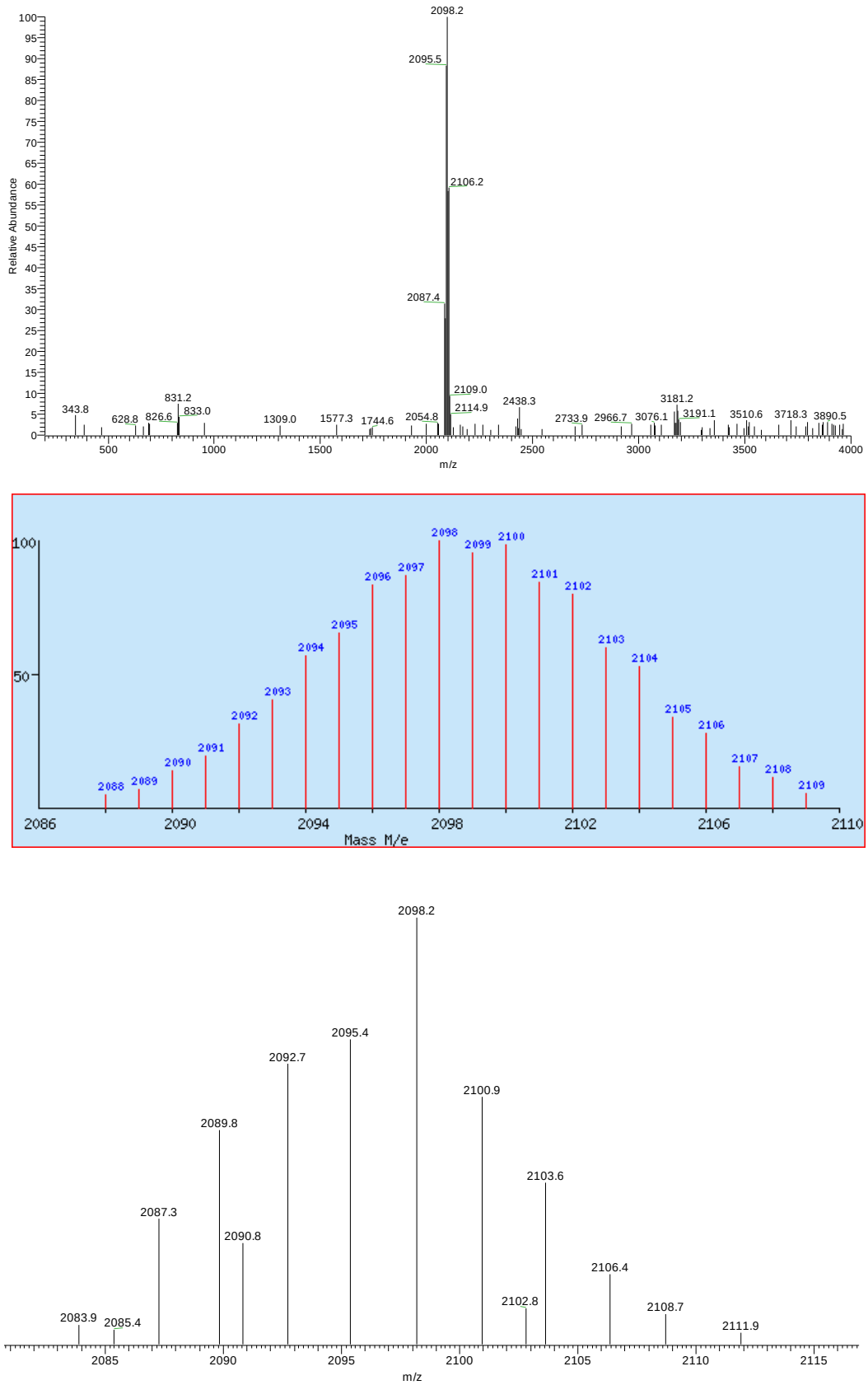

Figure S2. The negative-ion ESI mass spectrum of **2** (upper), and the calculated (middle) and the observed (lower) isotopic patterns for $[(TpMoS_3)_2Cu_7I_6(MeCN)_2]^{2-}$ dianion.

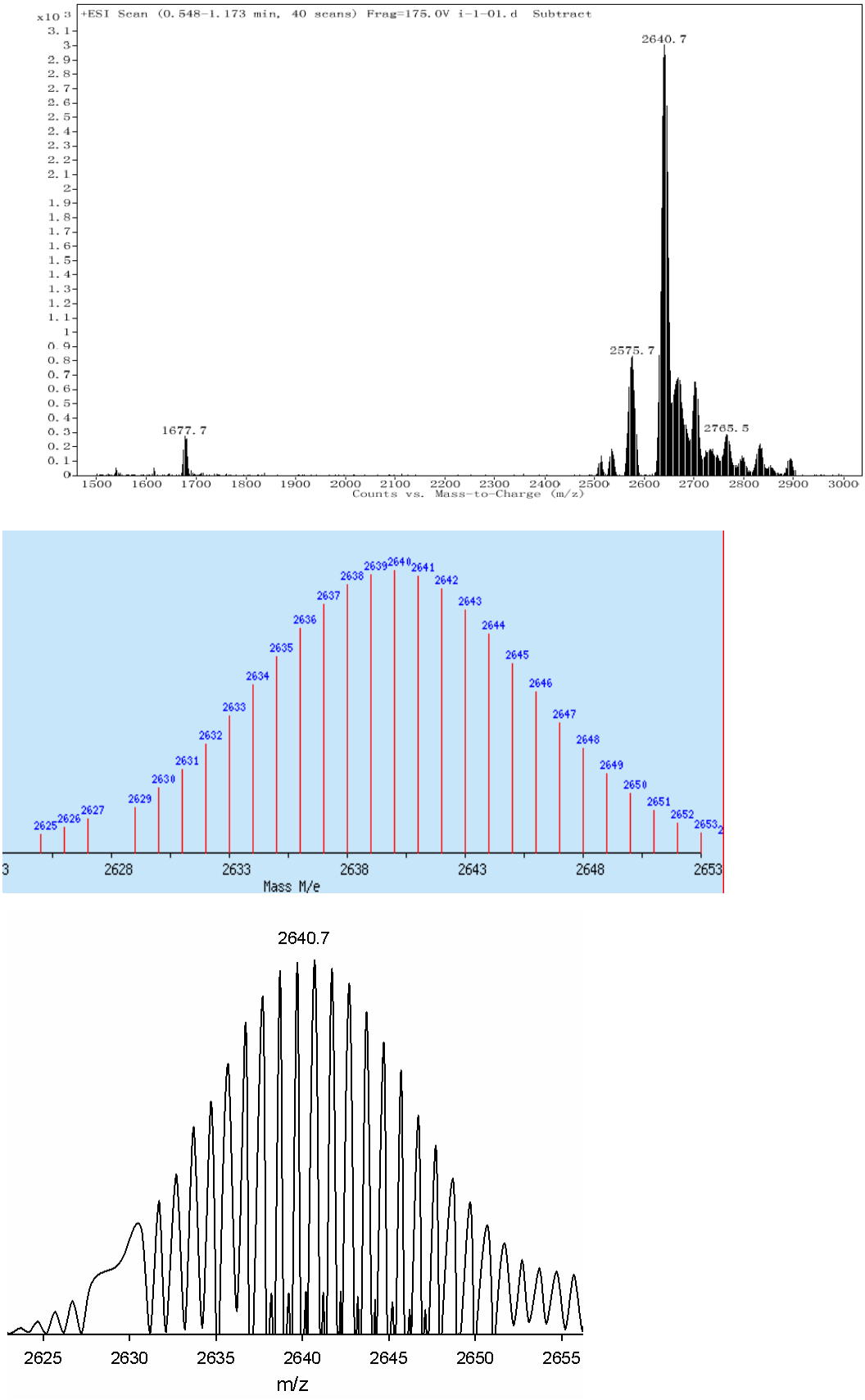

Figure S3. The negative-ion ESI mass spectrum of **3** (upper), and the calculated (middle) and the observed (lower) isotopic patterns for $\{[(TpMoS_3Cu_3)_4(\mu_3\text{-}S)_4](\mu_{12}\text{-}I)\}^-$ anion.

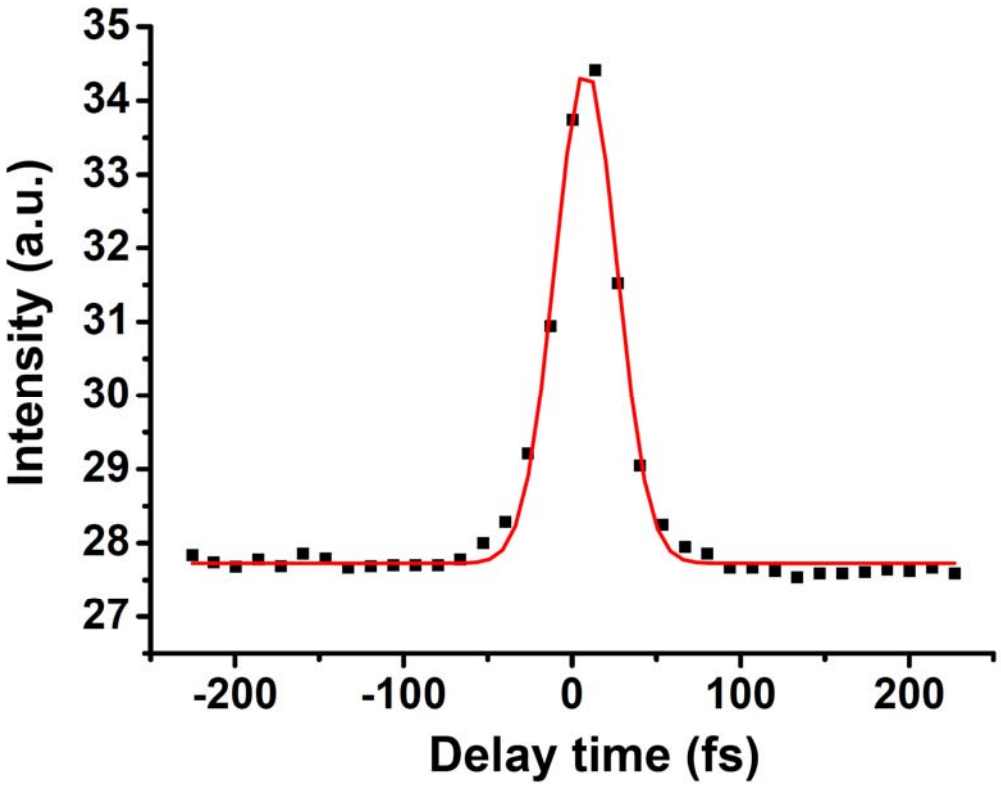

Figure S4. The DFWM signal for the DMF solution of 1.0×10^{-4} M for **2** with 80 fs laser and 1.5mm cell. The black solid squares are experimental data, and the red solid curves are the theoretical fit.

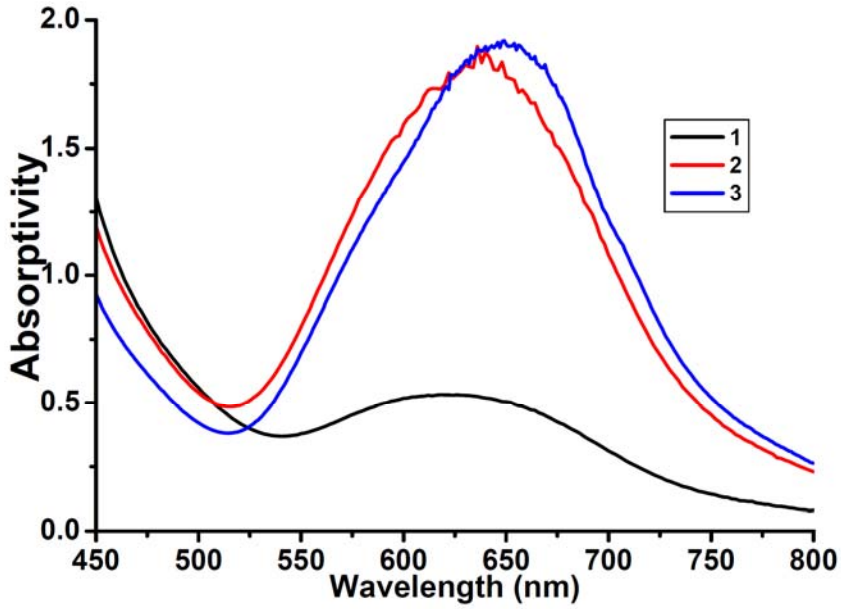

Figure S5. Electronic spectra of **1** (1.5×10^{-5} M), **2** (1.5×10^{-5} M) and **3** (1.5×10^{-5} M) in DMF in a 1-cm-thick glass cell.